ACUSTICA
S. HIRZEL VERLAG · STUTTGART
Volume 53 1983 No. 5

A Neural-Counting Model Incorporating Refractoriness and Spread of Excitation: III. Application to Intensity Discrimination and Loudness Estimation for Variable-Bandwidth Noise Stimuli

by M. C. Teich
Columbia University, Department of Electrical Engineering, New York, New York 10027
and G. Lachs
The Pennsylvania State University, Department of Electrical Engineering, University Park, Pennsylvania 16802

Summary

An energy-based neural-counting model, incorporating refractoriness and spread of excitation, has recently been applied by the authors to intensity discrimination and loudness estimation for pure-tone stimuli. We now examine the behaviour of this model when the stimulus is variable-bandwidth noise rather than a pure tone. The theoretical predictions are in good agreement with existing psychophysical data for intensity discrimination and loudness estimation. The functional dependence of the theoretical intensity discrimination and loudness curves on the noise bandwidth is established by the tuned-filter characteristics of the neural channels in conjunction with the spectral properties of the stimulus. No appeal to stimulus intensity fluctuations or to external critical bands is made in carrying out our analysis.

Ein neurales Zählmodell, welches die Refraktärzeit und die Verbreiterung der Erregung einbezieht: III. Anwendung zur Intensitätsunterscheidung und Lautheitsschätzung für Rauschen veränderlicher Bandbreite

Zusammenfassung

Ein energiebezogenes neurales Zählmodell, welches die Refraktärzeit und die Verbreiterung der Erregung berücksichtigt, wurde kürzlich vom Autor zur Intensitätsunterscheidung und Lautheitsschätzung von reinen Tönen als Reizen angewandt. Nunmehr wird das Verhalten dieses Modells bei Reizen untersucht, die aus Rauschen mit variabler Bandbreite bestehen. Die theoretischen Vorhersagen stimmen gut mit vorliegenden psychophysikalischen Daten für die Intensitätsunterscheidung und die Lautheitsschätzung überein.

Die funktionale Abhängigkeit der theoretischen Intensitätsunterscheidung und der Lautheitskurven von der Bandbreite des Rauschens wird hervorgerufen durch die „tuned-Filter"-Charakteristik der neuralen Kanäle in Verbindung mit den spektralen Eigenschaften des Reizes. Bei der Durchführung dieser Analysen blieben sowohl Intensitätsschwankungen des Reizes als auch die kritischen Bänder unberücksichtigt.

Un modèle à comptage d'impulsions nerveuses incorporant le phénomène de phase réfractaire et l'étalement de l'excitation: III. Application à la discrimination d'intensité et à l'estimation de sonie de bruits à largeur de bande variable

Sommaire

Les auteurs ont récemment appliqué à la discrimination d'intensité et à l'estimation de sonie des sons purs un modèle de comptage des impulsions nerveuses basé sur des considérations d'énergie et prenant en compte l'effet de la phase réfractaire ainsi que l'étalement de l'excitation le long de la membrane basilaire. Ils étendent ici ce modèle aux cas où les stimuli ne sont plus des sons purs mais des bruits de largeurs spectrales quelconques.

Les prédictions théoriques obtenues ici sont en bon accord avec les résultats expérimentaux établis antérieurement par divers auteurs aussi bien pour l'estimation de sonie que pour la discrimination d'intensité. Les relations fonctionnelles reliant la discrimination d'intensité théorique et les courbes de sonie à la largeur spectrale du bruit reposent sur les caractéristiques de filtres adaptés des canaux nerveux en relation avec les propriétés spectrales du stimulus. La présente analyse ne fait appel ni aux fluctuations d'intensité du stimulus ni à la notion de bande critique.

1. Introduction

This is the third in a series of papers. In Part I (Teich and Lachs [1], denoted I) we demonstrated that an energy-based neural counting model incorporating refractoriness (dead time) and spread of excitation satisfactorily described the results of pure-tone intensity discrimination experiments. In Part II (Lachs and Teich [2], denoted II) we showed that the identical linear filter refractoriness model (LFRM) also provided proper results for pure-tone loudness estimation experiments at all stimulus levels. In particular, as the stimulus intensity is increased from very low to moderate values, the model predicts that the slope of the intensity discrimination curve climbs from 1/2 towards unity, whereas the slope of the loudness function gradually declines below 1 in this same region. For sufficiently high values of the stimulus intensity, the slopes calculated from a simplified (crude saturation) version of the model are found to be $1-1/4N$ for the intensity discrimination curve and $1/2N$ for the loudness function. The quantity N is the number of pairs of complex poles associated with the tuned-filter characteristic of the individual neural channels; it is the only important free parameter in the model[1]. Appropriate values for N were found to lie between 2 and 4, providing an asymptotic slope for the intensity discrimination curve bounded by 7/8 and 15/16 and an asymptotic slope for the loudness function bounded by 1/4 and 1/8. Our model implies that a single theoretical mechanism mediates both pure-tone intensity discrimination and loudness estimation. The near-miss to Weber's Law and Stevens' Power Law emerge naturally along the way.

Having investigated the performance of the LFRM for intensity discrimination and loudness estimation in the pure-tone case, it is natural to consider whether it is also useful for other stimuli. In this work, we demonstrate that it is indeed useful when the stimulus is variable-bandwidth white noise. In Section 2 we describe the model. The theoretical results are compared with experimental data for loudness estimation and intensity discrimination in Section 3, and the results are discussed in Section 4.

2. Model

Fig. 1 is a block diagram for the LFRM reproduced from papers I and II, where the elements of the model have been described in detail. The output of the decision centre represents either loudness estimation or intensity discrimination, as the paradigm dictates. All neural channels are assumed to be independent in this energy-based model.

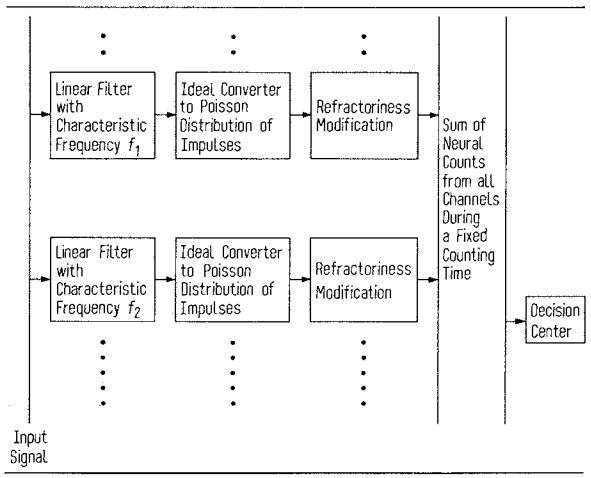

Fig. 1. Block diagram for linear filter refractoriness model (LFRM).

For loudness, we consider a scalar loudness random variable given by (see II)

$$\mathscr{L} = \varkappa X . \tag{1}$$

The quantity X is a discrete random variable, well represented by a Gaussian distribution, expressing the total number of neural counts from all channels in the fixed counting time T; $\varkappa$ is a constant. In our characterization, we assume that the estimates are statistically independent from trial to trial, and that the loudness function L is obtained by forming the expectation $\mathscr{E}(\cdot)$ of eq. (1), i.e.,

$$L = \mathscr{E}(\mathscr{L}) = \varkappa \mathscr{E}(X) = \varkappa \bar{N}_c . \tag{2}$$

Here $\bar{N}_c \equiv \mathscr{E}(X)$ is the overall mean neural count. The notation is identical to that used in I and II.

The typical intensity-discrimination experiment employs a two-interval forced choice (2IFC) procedure in which the subject is sequentially presented with two short stimulus bursts at different levels. The level of one burst is fixed while the level of the other is adjusted until the subject makes a correct decision on a pre-specified percentage of the trials. An appropriate quantitative measure for this experiment in the context of the LFRM is a detection distance h given by (see I)

$$h = \frac{\mathscr{E}(X_s) - \mathscr{E}(X_w)}{[\sigma^2(X_s) + \sigma^2(X_w)]^{1/2}} . \tag{3}$$

Here $\mathscr{E}(X_s)$, $\sigma^2(X_s)$ and $\mathscr{E}(X_w)$, $\sigma^2(X_w)$ are the mean and variance of the total number of neural counts for the stronger and weaker inputs, respec-

[1] In Parts I and II (Teich and Lachs [1, 2]), we rather loosely referred to N as the number of poles, rather than as the number of pairs of complex poles. Thus, $N=2$ corresponds to a system consisting of 2 pairs of complex poles, which represents a fourth-order system (an example is the series connection of 2 tuned circuits).

tively. The quantity h is selected to satisfy the specified criterion for the probability of making a correct decision. As an example, let's suppose that the stronger input level is fixed, and the level of the weaker input is adjusted to satisfy eq. (3). This procedure provides one data point. Other data points are obtained by selecting different values for the intensity of the stronger input (keeping h constant), and repeating the process of varying the weaker level until eq. (3) is satisfied.

The LFRM accounts for spread of excitation by assigning an N-pole-pair tuned linear-filter characteristic to the frequency response of each neural channel, and it employs fixed non-paralyzable dead-time (refractoriness) as a simple saturation mechanism. Thus, the number of neural impulses observed in the counting (observation) time T, and the mean and variance of this quantity which appear in eqs. (2) and (3), involve refractoriness-modified counting statistics. The overall dead-time-modified mean $\bar{N}_c$ and variance Σ_c^2, of the number of neural counts, are given by the following approximate formulas when the inputs are non-random (see I and II):

$$\bar{N}_c = A' \int_{f_L}^{f_U} \frac{E(f_0)\,df_0}{1 + A' E(f_0)(\tau/T)} \tag{4}$$

and

$$\Sigma_c^2 = A' \int_{f_L}^{f_U} \frac{E(f_0)\,df_0}{[1 + A' E(f_0)(\tau/T)]^3}\,. \tag{5}$$

The quantities f_L and f_U represent the lower and upper frequency limits of the auditory response, respectively, $E(f_0)$ is energy output of a linear filter (which may have non-symmetric response) whose characteristic or best frequency is f_0, τ is the dead-time interval, and A' is a fixed proportionality constant that relates counts to energy at the ideal Poisson converter (see Fig. 1).

A non-symmetric filter response yields the following form for $E(f_0)$

$$E(f_0) = A_1 \int_{f_L}^{f_0} \frac{S(f)\,df}{[1 + Q^2(f/f_0 - f_0/f)^2]^N} + A_1 \int_{f_0}^{f_U} \frac{S(f)\,df}{[1 + Q^2(f/f_0 - f_0/f)^2]^{rN}}\,. \tag{6}$$

Here $S(f)$ represents the energy spectral density of the input signal and A_1 is a constant that is eventually absorbed into A' of eqs. (4) and (5). The filter is assigned an N-pole roll-off for $f < f_0$ and an rN-pole roll-off for $f > f_0$, for reasons described in I and II. The parameter Q is the usual 3-dB Q for a single-pole-pair tuned filter. A symmetric filter response is obtained by setting $r = 1$. When the stimulus consists of short bursts, as is the case in all of the experiments considered here, its magnitude may be expressed in terms of energy (E), power (P), or intensity (I).

Loudness and intensity discrimination for general input signals may be examined by using eqs. (4) to (6) in eqs. (2) and (3), respectively. In the special case of a pure-tone signal

$$S(f) = E_T\,\delta(f - f_T)\,, \tag{7}$$

where E_T and f_T represent the energy and frequency of the tone, respectively. Substituting eq. (7) into eqs. (2) to (6) leads to the results described previously (see Parts I and II). For an input signal consisting of several tones, the energy spectrum is easily written as a summation of several terms such as those represented in eq. (7), but care must be taken to incorporate the effects of combination tones generated in the ear. We have investigated input signals of this type in connection with tone masking, and will report the results in a forthcoming paper.

The stimulus we consider in detail in this paper is band-limited noise. The mathematical results derived in this section may be directly applied to noise stimuli, provided that the average energy and spectral density (rather than the energy fluctuations of the stimulus) are the crucial determinants for intensity discrimination and loudness estimation. We believe that this is an appropriate assumption (see Section 4) and therefore proceed by inserting the following spectral density

$$S(f) = \begin{cases} \eta, & f_1 \leqq f \leqq f_2 \\ 0, & \text{otherwise} \end{cases} \tag{8}$$

in eq. (6). Here η is the average noise energy per cycle of bandwidth (Hz), and f_1 and f_2 represent, respectively, the lower and upper cut-off frequencies for the noise stimulus. The evaluation of eq. (6) for the input spectrum represented by eq. (8) is carried out in Appendix A. This result is then utilized in the numerical calculation of the integrals in eqs. (4) and (5) which, in turn, provide the LFRM predictions for loudness and intensity discrimination. The results of our model are compared with various experimental data in the next section.

Before proceeding, however, it is interesting to point out that an analytical result can be obtained for the intensity-discrimination law in the limit of strong broadband stimuli of arbitrary spectra, if the assumption is made that strong non-paralyzable dead time is the sole saturation mechanism. The derivation is carried out in Appendix B and leads to Weber's Law. The calculation is an extension of the

single-channel result first derived by van der Velden [4], and contains a number of limiting conditions. Each channel is assumed to be strongly saturated as a result of non-paralyzable dead-time. All channels are taken to be independent and their outputs summed. Finally, since all the neural channels are strongly saturated, the effects of spread of excitation are not experienced. In I it was shown that spread of excitation is a basic ingredient in the LFRM formulation that leads to the near-miss to Weber's Law for pure-tone inputs. A cautionary note regarding the blind use of these results must be sounded, however. Experimental results for the neural count mean and variance indicate that a more plausible modal must involve the effects of saturation as well as those of refractoriness.

3. Comparison with experimental data

3.1. Loudness summation for Gaussian noise stimuli

We first examine the behaviour of the LFRM in the context of loudness summation data. These data are usually represented in the form of sound pressure level for an equivalently loud pure tone or prespecified band of noise, versus the half-power bandwidth of the noise stimulus ΔF. Filtered Gaussian noise is used as the stimulus, and its total energy is constrained to be constant. Thus, as an example, when the bandwidth is doubled, the energy density is halved. The energy density is usually centred geometrically about a given frequency, and the comparison tone frequency (or the geometric mean of the comparison noise band) is chosen to be the same as the geometric mean of the stimulus band. Experimental studies of this kind were first carried out by Zwicker and Feldtkeller [5], Feldtkeller and Zwicker [6], and Zwicker, Flottorp, and Stevens [7].

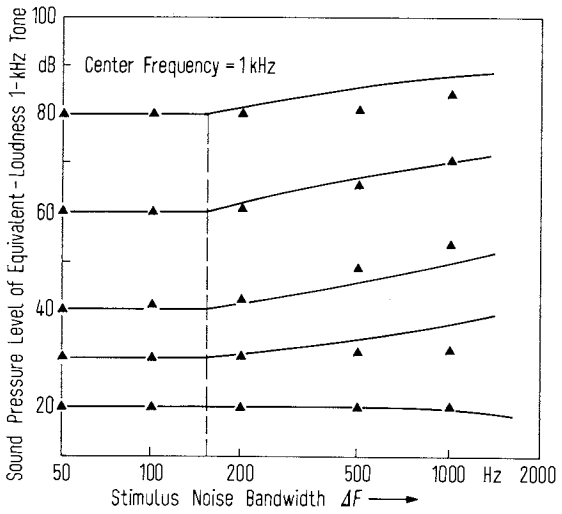

Fig. 2. Solid curves show the dependence of loudness on the bandwidth ΔF of filtered white Gaussian noise of centre frequency 1 kHz. The total noise energy was maintained constant for each curve. The subjects adjusted the SPL of a 1-kHz pure tone to match the loudness at each noise bandwidth ΔF. Experimental data adapted from Fig. 21.1 of the book by Feldtkeller and Zwicker [6]. The solid triangles represent the predictions of the LFRM for the $N = 2$ case. They are seen to follow the trends of the curves at all sound pressure levels.

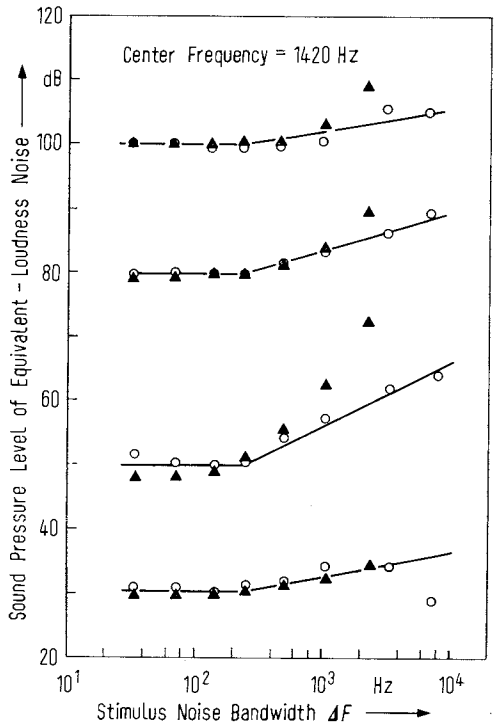

Fig. 3. Open circles (and straight-line segments fitted to them) show the dependence of loudness on the bandwidth ΔF of filtered Gaussian noise of centre frequency 1420 Hz. The total noise energy was maintained constant for each curve. The subjects adjusted the SPL of a band of noise of center frequency 1420 Hz and bandwidth 210 Hz to match the loudness at each noise bandwidth ΔF. Experimental data (open circles and solid curves) adapted from Fig. 8 of the paper by Zwicker, Flottorp, and Stevens [7]. The solid triangles represent the predictions of the LFRM for the $N = 2$ case. As observed in Fig. 2, they follow the trends of the curves at all sound pressure levels.

In Fig. 2 we present a set of such data (solid curves) reported by Feldtkeller and Zwicker ([6], Fig. 21.1, p. 82) for a 1-kHz comparison tone. Fig. 3 shows a similar set of data (open circles and solid curves) reported by Zwicker, Flottorp, and Stevens ([7], Fig. 8, p. 553); in this case, a band of noise of centre frequency 1420 Hz and half-power bandwidth 210 Hz served as the comparison. The theoretical predictions of the LFRM are represented by the solid triangles in Figs. 2 and 3 for the $N = 2$ case. Because we are dealing with a matching paradigm, the values of the model parameters B_1 and

B_2 (see II) are not critical. They are chosen to be of similar magnitude to those used in the pure-tone case, and to give a loudness of approximately 1 (sone) for narrowband noise at the 40-dB intensity level. In particular, the values used for both Figs. 2 and 3 were $B_1 = 4.668 \times 10^{-6}$ and $B_2 = 1.000 \times 10^{-3}$. The parameter $Q_{10\,\mathrm{dB}}$ was set equal to 4; this provided a reasonably good fit to both sets of data.

As pointed out in II, it must be kept in mind that the model constants providing a good fit to the empirical data, for the simple LFRM presented here, will change when the details of the peripheral auditory system are incorporated into the model.

The experimental data show that loudness increases with the bandwidth ΔF even though the total stimulus energy is maintained constant. This so-called loudness summation effect (LSE) represents interesting and important behaviour. From Figs. 2 and 3, it is clear that the LSE is substantially smaller for both low and high stimulus energies than it is for intermediate stimulus energies. Furthermore, the effect does not seem to occur until a particular bandwidth is achieved (indicated by the breakpoints in the solid curves). This behaviour is generally ascribed to the existence of critical bands (Fletcher [8]; Zwicker and Feldtkeller [5]; Feldtkeller and Zwicker [6]; Zwicker, Flottorp, and Stevens [7]; Scharf [9, 10]; Zwislocki [11]).

The theoretical calculations based on the LFRM (indicated by the solid triangles in Figs. 2 and 3) clearly follow the general trend of the experimental data. A substantially larger LSE is predicted for intermediate stimulus energies than for low and high stimulus energies, though the magnitude of the predicted effect is too large at the upper values of ΔF. It is important to note that the LFRM calculations also mimic the experimental results relating to the bandwidth value at which the LSE becomes significant.

The behaviour of the LFRM may be understood in terms of refractoriness and spread of excitation as follows. At low stimulus levels, refractoriness is absent and the overall neural-count random variable is Poisson. Its mean and variance are governed purely by the total energy passed through the bank of linear filters. Since this energy is independent of ΔF, there is no loudness summation. In this region, the loudness function will exhibit unity slope regardless of the stimulus bandwidth (see II).

For noise stimuli of intermediate level, neural channels within the stimulus bandwidth will be saturated only for narrow bandwidths. If the bandwidth is increased while the energy is maintained constant, the decrease in energy density results in the individual channels being less saturated. Thus, the total neural count, and therefore the perceived loudness, increases with increasing ΔF. In this region, the slope of the loudness function remains unity for broadband stimuli but falls below unity for narrowband stimuli (see II). This is illustrated vividly in Fig. 4, which presents loudness functions generated by the LFRM for values of the stimulus noise bandwidth ranging from $\Delta F = 35$ Hz (narrowband) to $\Delta F = 7500$ Hz (broadband). All of the other model parameters are identical with each other, and with those used in Fig. 3 ($f_0 = 1420$ Hz, $N = 2$, $Q_{10\,\mathrm{dB}} = 4$, $B_1 = 4.668 \times 10^{-6}$, $B_2 = 1.000 \times 10^{-3}$). The narrowband curve has a behaviour virtually indistinguishable from that of a 1-kHz pure-tone loudness function, including the power-law behaviour at intensity levels above 35 dB SPL (see II), whereas the broadband curve displays the more rounded appearance that is characteristic of experimental loudness functions for broadband noise (see, e.g., [6], Fig. 21.4; [10], Fig. 7). This occurs because of the expanded range of unity slope (up to about 35 dB SPL in Fig. 4), and the later onset of saturation. Furthermore, because of the reduced overall saturation, the LFRM predicts that

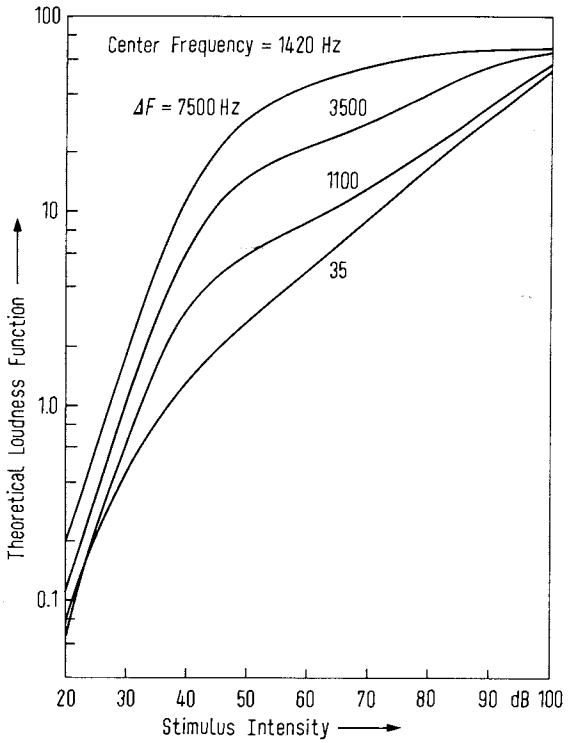

Fig. 4. Theoretical loudness functions for Gaussian noise of various bandwidths versus total stimulus energy (intensity) in dB. The curves have been generated by the LFRM with all parameters identical except ΔF. The (geometric mean) frequency is 1420 Hz and the parameter $N = 2$. The characteristic features of the narrowband and broadband curves are in accord with experiment.

broadband noise will elicit a substantially greater loudness sensation for most stimulus levels, with the maximum advantage occurring at about 50 dB SPL (see Fig. 4). This behaviour is also in accord with experiment (Brittain [12]; Stevens [13]; Zwicker [14]; Zwicker [15]). Theoretical loudness functions for intermediate bandwidths fall between the two extremes, exhibiting one or more points of inflection.

Finally, at high stimulus levels, the channels within the stimulus bandwidth remain saturated in spite of the bandwidth increasing. Thus, the overall neural count will grow as the stimulus bandwidth is increased (see Figs. 2 and 3), but not as rapidly as if the saturation were alleviated by the increase in ΔF. Spread of excitation causes the pure-tone loudness function to increase in accordance with Stevens' power law in this region (see II). The noise loudness function, on the other hand, grows more slowly because the channels are more saturated and less spread of excitation is available. The behaviour of the slope of the broadband-stimulus loudness function in this region is determined by eq. (B. 3) and the expansion $\lg(1+x) \cong x$ for $|x| \ll 1$.

3.2. *Intensity discrimination for Gaussian noise stimuli*

We now examine the behaviour of the LFRM in the context of intensity discrimination. These data may be displayed in a number of ways; the most usual presentation is as a plot of $\lg \Delta I$ versus $\lg I$, or of $\lg (\Delta I/I)$ versus $\lg I$. Filtered Gaussian noise is used as the stimulus. The energy density is usually centred geometrically about the centre frequency and is identical in form in both intervals of the two-interval forced-choice procedure. The earliest experimental study of this kind was carried out by Miller [3], for broadband Gaussian noise stimuli. Related studies were conducted by Hawkins and Stevens [16], Zwicker [17], Bos and de Boer [18], and Raab and Goldberg [19], among others.

In Fig. 5 we present a set of such data in the form of a plot of $\lg (\Delta I/I)$ versus $\lg I$ (open circles and straight-line segments connecting them), reported by Bos and de Boer ([18], Fig. 5, p. 711)[2]. The stimulus consisted of Gaussian noise bursts of 125 ms duration with a (geometric mean) frequency of 1 kHz and a bandwidth of 800 Hz. Bos and de Boer carried out their measurements in the presence of a weak broadband background noise, the magnitude of which was chosen in an attempt to eliminate off-frequency listening and spread of excitation (thereby

[2] To make contact with the notation used by Bos and de Boer [18], note that our I is their I_0 and our ΔI is their I_1.

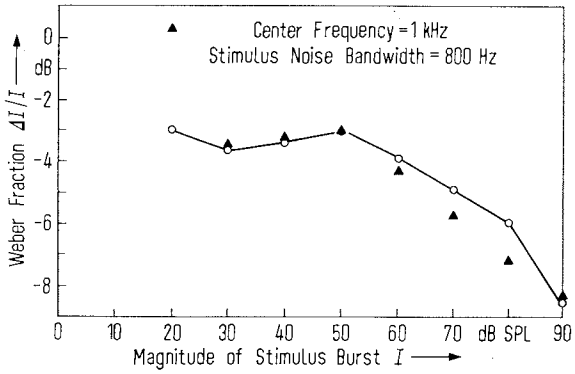

Fig. 5. Open circles (and straight-line segments connecting them) display the Weber fraction $\Delta I/I$ (in dB) versus the power ratio per 1/3 octave of the stimulus burst I (in dB re 0.0002 μbar). The Gaussian noise stimulus has a (geometric mean) frequency of 1 kHz, a bandwidth of 800 Hz, and a duration of 125 ms. A very weak broadband background noise (−30 dB re I) was also present. Experimental data adapted from Fig. 5 of the paper by Bos and de Boer [18]. The solid triangles represent the predictions of the LFRM for the $N=2$ case (theory and experiment are matched at 50 dB SPL). The theoretical results follow the trend of the experimental data very well.

leading to Weber's Law). For the particular data set illustrated, however, this noise was sufficiently weak (−30 dB re I) that it most likely can be ignored.

The theoretical predictions of the LFRM with $N=2$ are represented by the solid triangles in Fig. 5, when the stimulus has the same (geometric mean) frequency of 1 kHz and a bandwidth of 800 Hz. The weak broadband noise was omitted from the theory. The model parameters were selected to be $Q_{10\,\mathrm{dB}}=4$, $\tau/T=0.05$, and $h=1$, which are similar to those used in our other studies. As we observed in Paper I, the slope of the theoretical intensity-discrimination curve is relatively independent of the choice of these parameters. The quantity A' appearing in eqs. (4) and (5) was chosen in such a way that the calculated value of $\lg (\Delta I/I)$ at $I=$ 50 dB SPL was equal to the experimental value, viz., −3 dB. As in the case of loudness, discussed earlier, the optimal model constants will change when the details of the peripheral auditory system are incorporated into the LFRM.

The experimental data show that $\lg (\Delta I/I)$ is relatively flat with I (i.e., Weber's Law is approximately obeyed), for 20 dB SPL $\leq I \leq$ 50 dB SPL. A slight dip does appear in the data at 30 dB, however. For 50 dB SPL $\leq I \leq$ 80 dB SPL, the data lie on a line whose slope is about −0.1. In terms of the standard intensity-discrimination curve ($\lg \Delta I$ versus $\lg I$), this corresponds to a slope of 0.9, representing the near miss to Weber's Law. This is the

same behaviour as that observed for pure-tone intensity discrimination, but we note that the onset of the near miss occurs at a higher value of I for the 800-Hz bandwidth noise than it does for a pure tone (see Paper I; Rabinowitz et al. [20]; Jesteadt et al. [21]). Bos and de Boer ([18], Fig. 5, p. 711) also carried out intensity-discrimination experiments for a noise stimulus with a centre frequency of 1 kHz, and a bandwidth of 200 Hz. A near miss to Weber's Law (with slope $\cong -0.1$) is also observed in that case, and the onset is at a lower value of I than for the 800 Hz bandwidth data. The intensity-discrimination behaviour for noise is sometimes ascribed to the existence of intensity fluctuations (Green [22]; Jeffress [23]; Pfafflin and Mathews [24]; de Boer [25]; McGill [26]; Ronken [27]; Teich and McGill [28]), and sometimes to other factors (Green and Swets [29], pp. 225–229).

The theoretical calculations based on the LFRM (solid triangles in Fig. 5) are in good agreement with the trend of the experimental data. The principal discrepancy is at the lowest intensity-level data point ($I = 20$ dB SPL). The behaviour of the LFRM for intensity discrimination may be understood in terms of refractoriness and spread of excitation. At the lowest levels of excitation, refractoriness is absent, and the overall neural-count random variable is Poisson regardless of the stimulus noise bandwidth ΔF. This gives rise to the de Vries-Rose Law, yielding a slope of -0.5 for the lg $(\Delta I/I)$ versus lg I curve (see I). In this region, the loudness function exhibits unity slope.

For noise stimuli of intermediate level, neural channels within the stimulus bandwidth will remain unsaturated for broad bandwidths, and the de Vries-Rose Law will persist. If the stimulus bandwidth is decreased while the energy is maintained constant, however, the increase in energy density will result in the individual channels being more saturated. This drives the intensity discrimination behaviour toward Weber's Law (in accordance with the calculations of van der Velden [4], Bouman, Vos, and Walraven [30], and those presented in Appendix B) or toward whatever law a specific saturation function may specify. In this region, the slope of the loudness function falls below unity.

At high stimulus levels, spread of excitation can occur only for narrowband stimuli, where unsaturated channels are available beyond the saturated excitation region. Thus, just as for the pure-tone case treated in Paper I, the near miss to Weber's Law will take over for small ΔF, and the loudness function will obey Stevens' power Law. For broadband stimuli, where all channels are saturated, the neural count will continue to grow, but spread of excitation can not take place and Weber's Law will persist (see Appendix B).

The theoretical results are in good qualitative agreement with available data for Gaussian noise stimuli. Miller's ([3], Fig. 3) broadband intensity discrimination data can be interpreted as obeying the de Vries-Rose Law at the lowest levels of intensity, making a smooth transition to Weber's Law, which takes over fully at about 30 dB SL. The near-miss is never observed. Bos and de Boer's ([18], Fig. 5) $\Delta F = 800$ Hz data approximately obey Weber's Law from about 20 to 50 dB SPL, and follow the near miss above 50 dB SPL. Bos and de Boer's ([18], Fig. 5) $\Delta F = 200$ Hz data appear to obey Weber's Law between 10 and 20 dB SPL, and then follow the near miss above 20 dB SPL.

4. Discussion

We have found that the predictions of an energy-based neural-counting model, incorporating refractoriness and spread of excitation, are in good accord with psychophysical data for loudness estimation and intensity discrimination. This is true both for the variable-bandwidth Gaussian noise stimuli studied here, and for the pure-tone stimuli studied previously (Teich and Lachs [1]; Lachs and Teich [2]). We have appealed neither to external critical bands nor to stimulus intensity fluctuations in carrying out our study.

Our model makes use only of the energy spectral density of the signal, so that we will want to know its applicability for stimuli of various statistical properties. A number of intensity-discrimination studies using non-pure-tone, non-Gaussian stimuli have been carried out. The agreement of the LFRM calculations with most of these experimental results appears to provide a sound basis for a broad applicability of the theory, as discussed in the following.

Miller [3], in his classic study, performed intensity-discrimination experiments using not only broadband Gaussian noise, but also Gaussian noise in which the peak amplitudes were clipped at a fixed level (see Fig. 3 in his paper). The outcome of both sets of experiments are indistinguishable; the data obey the de Vries-Rose Law at the lowest stimulus levels making a smooth transition to Weber's Law, which takes over fully at about 30 dB SL. Penner and Viemeister [31] studied the intensity discrimination of filtered clicks. For two of the three subjects they tested, the data for broadband clicks ($\Delta F = 10$ kHz; see Fig. 2 in their paper, S 1 and S 3) are virtually identical to the Miller data: a transition from the de Vries-Rose Law to Weber's Law occurs at about 30 dB SL. For narrowband clicks

($\Delta F = 780$ Hz, Fig. 1), the near miss to Weber's Law (with a slope of about 0.92) takes over at moderate stimulus levels, just as in the Bos and de Boer data for narrowband Gaussian noise ($\Delta F = 800$ Hz, Fig. 5). Raab and Goldberg [19] investigated intensity discrimination using bursts of variable-bandwidth reproducible Gaussian noise. Weber's Law was clearly obeyed for broadband noise of this character ($\Delta F = 5$ kHz, Table III); the near miss appeared to emerge for narrowband reproducible noise ($\Delta F = 500$ Hz, Table III).

Quite a few intensity-discrimination studies were conducted in the presence of background noise of various kinds. Bos and de Boer ([18], Fig. 5) showed that broadband Gaussian background noise drove the intensity discrimination curve for a narrowband Gaussian noise stimulus away from the near miss toward Weber's Law, and generally degraded performance by increasing the Weber fraction. Similar results were demonstrated for band-reject background noise by Viemeister [32], and by Moore and Raab [33]. Viemeister [34], and Moore and Raab [35], had earlier demonstrated that the slope of the pure-tone intensity-discrimination curve was driven toward unity by the presence of Gaussian background noise of various spectral properties. Broadband background noise also degraded the Weber fraction for click intensity discrimination, according to Penner and Viemeister [31], but Weber's Law again held fast.

All of these results can be understood in a uniform way, in terms of the LFRM. Saturated channels, however few or many there may be, and at whatever frequencies they are excited, give rise to Weber's Law because of saturation and refractoriness effects. Unsaturated (off-frequency) channels will, when they are excited, reduce the slope of the intensity-discrimination curve below unity. The slope of the near miss is determined by the slopes of the tuning-curve tails. The use of broadband signals, or the presence of background stimuli, of whatever spectral distribution and statistical nature, will reduce the number of unsaturated channels and drive the intensity-discrimination curve toward Weber's Law. Of course, the magnitude of the Weber fraction will depend on the extent of the saturation which, in turn, is determined by the signal and background.

That is not to say that intensity fluctuations are altogether unimportant in intensity-discrimination tasks. Experiments such as those carried out by Ronken [27] and Spiegel and Green [36] indicate that intensity fluctuations do play a part, and we know how to deal with them analytically (Prucnal and Teich [37]). But their importance will diminish as the time-bandwidth product increases, because of the averaging of the (energy) fluctuations (Green [22]; Green and Swets [29]; McGill [26]; Sorkin, Woods, and Boggs [38]; Papoulis [39], pp. 378–381), because of saturation (Siebert [40]), and because of refractoriness effects (Vannucci and Teich [41]).

The loudness function is simpler, in that it depends only on the mean neural count, and not on the count variance. As such, it provides a less discriminating window on system operation. In any case, the LFRM provides results that follow the general trends of loudness summation data, without appealing to an ad-hoc critical-band concept. We do not imply that critical bands are unimportant in this task, however. Scharf [10] has discussed various models of loudness that make use of the critical-band concept and provide very good agreement with experimental data. Zwicker and Scharf [42], in particular, have developed a model for loudness summation, incorporating Stevens' power Law and critical bands (see also [15]), that is eminently successful. Our results do suggest, however, that much of the behaviour of loudness summation can be understood rather simply in terms of saturation due to refractoriness and spread of excitation arising from the tuned-filter characteristics of the neural channels.

Finally, we reiterate that many known physiological characteristics of the peripheral auditory system have been omitted from our model. These include the energy distribution along the cochlear partition, the approximately logarithmic relationship between distance along the basilar membrane and best frequency, the nonlinear receptor response, the nonuniform fibre innervation density, and the nonlinear (with stimulus intensity) active fibre density arising from the spread in range over which different fibres initiate firing. Other relevant factors are symmetric versus nonsymmetric linear-filter characteristics, monaural versus binaural processing, spontaneous counts, the occurrence of phase locking, the existence of relative refractoriness (Teich and Diament [43]), and the middle-ear transmission characteristic. We are in the process of incorporating a number of these properties into a more comprehensive model, on which we shall report shortly.

The character of the predictions, as reported here, appear to be left basically unchanged by the additions though the detailed predictions of the model accord better with experiment. This provides us with a measure of confidence that the essential effects of saturation and refractoriness, along with spread of excitation, capture the response of the auditory system in the simple psychophysical tasks discussed in this paper.

A preliminary account of this work was reported at the 1981 Meeting of the Acoustical Society of America in Ottawa, Ontario [44].

Acknowledgement

This work was supported by the National Science Foundation under Grant BNS80-21140.

Appendix A
Evaluation of linear-filter energy output for band-limited noise input

We evaluate the total energy (intensity) at the output of an rN-pole-pair (possibly non-symmetric) linear filter [eq. (6)] stimulated by band-limited noise [eq. (8)]. The quantity η is the average noise energy per cycle of bandwidth (Hz), and f_1 and f_2 are, respectively, the lower and upper cut-off frequencies for the noise. Then, for a symmetric N-pole-pair linear filter with characteristic frequency f_0,

$$E(f_0) = A_1 \eta \int_{f_1}^{f_2} [1 + Q^2(f/f_0 - f_0/f)^2]^{-N} \mathrm{d}f. \quad (A.1)$$

Letting $x = f/f_0$ and $\mathrm{d}f = f_0 \mathrm{d}x$ provides

$$E(f_0) = A_1 \eta f_0 \int_{\alpha_1}^{\alpha_2} [1 + Q^2(x - 1/x)^2]^{-N} \mathrm{d}x, \quad (A.2)$$

where $\alpha_1 = f_1/f_0$ and $\alpha_2 = f_2/f_0$.

We then substitute

$$z = 1 + Q^2(x - 1/x)^2 \quad (A.3)$$

so that for

$$x > 1 \quad (A.4)$$

we obtain

$$(z-1)^{1/2}/Q = x - 1/x. \quad (A.5)$$

This is a quadratic equation with the solution

$$x = [(z-1)^{1/2} + (z - 1 + 4Q^2)^{1/2}]/2Q \quad (A.6)$$

which provides

$$\mathrm{d}x = \mathrm{d}z[(z-1)^{-1/2} + (z - 1 + 4Q^2)^{-1/2}]/4Q. \quad (A.7)$$

Similarly, for

$$0 < x < 1 \quad (A.8)$$

we obtain

$$(z-1)^{1/2}/Q = 1/x - x. \quad (A.9)$$

In this case, the solution is

$$x = [(z - 1 + 4Q^2)^{1/2} - (z-1)^{1/2}]/2Q \quad (A.10)$$

providing

$$\mathrm{d}x = \mathrm{d}z[(z - 1 + 4Q^2)^{-1/2} - (z-1)^{-1/2}]/4Q. \quad (A.11)$$

When $x = 1$, $z = 1$. We also effect the substitutions

$$z_1 = 1 + Q^2(f_1/f_0 - f_0/f_1)^2 \quad (A.12a)$$

and

$$z_2 = 1 + Q^2(f_2/f_0 - f_0/f_2)^2. \quad (A.12b)$$

The division into two regions represented by eqs. (A. 4) and (A. 8) is necessitated by the double-valued nature of eq. (A. 3). Since the split occurs at $x = 1$, $(f = f_0)$, it is a simple matter to incorporate the effects of a non-symmetric roll-off of the form

$$N\text{-pole-pair for } f < f_0 \quad (A.13a)$$

and

$$rN\text{-pole-pair for } f > f_0. \quad (A.13b)$$

The equations above yield the following specific integrals for $E(f_0)$

i) Case 1 $(f_1 < f_2 < f_0)$:

$$E(f_0) = \frac{A_1 \eta f_0}{4Q} \cdot [{}_0I_N(z_2, z_1) - {}_{4Q^2}I_N(z_2, z_1)]; \quad (A.14)$$

ii) Case 2 $(f_1 < f_0 < f_2)$:

$$E(f_0) = \frac{A_1 \eta f_0}{4Q} [{}_0I_N(1, z_1) - {}_{4Q^2}I_N(1, z_1) + {}_0I_{rN}(1, z_2) + {}_{4Q^2}I_{rN}(1, z_2)]; \quad (A.15)$$

iii) Case 3 $(f_0 < f_1 < f_2)$:

$$E(f_0) = \frac{A_1 \eta f_0}{4Q} \cdot [{}_0I_{rN}(z_1, z_2) + {}_{4Q^2}I_{rN}(z_1, z_2)]. \quad (A.16)$$

In all cases

$${}_aI_N(b, c) \equiv \int_b^c z^{-N}(z - 1 + a)^{-1/2} \mathrm{d}z. \quad (A.17)$$

Eq. (A. 17) is evaluated using the recurrence relation (Gradshteyn and Ryzhik [45], p. 73)

$${}_aI_N(b, c) = \frac{(c - 1 - a)^{1/2}}{(N-1)(a-1)c^{N-1}} - \frac{(b - 1 + a)^{1/2}}{(N-1)(a-1)b^{N-1}} - \frac{(2N-3)}{(2N-2)(a-1)} {}_aI_{N-1}(b, c), \quad (A.18)$$

beginning with

$${}_aI_1(b, c) = \frac{2}{(1-a)^{1/2}} \{\tan^{-1}[(c - 1 + a)^{1/2}] - \tan^{-1}[(b - 1 + a)^{1/2}]\}, \quad a < 1 \quad (A.19)$$

or

$$ {}_aI_1(b,c) = \frac{1}{(a-1)^{1/2}} \ln \left\{ \frac{[(c-1+a)^{1/2} - (a-1)^{1/2}][(b-1+a)^{1/2} + (a-1)^{1/2}]}{[(c-1+a)^{1/2} + (a-1)^{1/2}][(b-1+a)^{1/2} - (a-1)^{1/2}]} \right\}, \quad a > 1. \tag{A.20} $$

This is not a difficult task since N and r are both small integers. The quantity desired, $E(f_0)$, is then obtained from eqs. (A. 14) to (A. 20).

Appendix B
Derivation of Weber's Law for broadband noise stimuli using refractoriness model

We obtain an analytical expression for the intensity-discrimination law in the limit of broadband stimuli of arbitrary spectra. Our point of departure is the first-order non-paralyzable dead-time-modified count mean and variance for a single channel. The appropriate expressions are (Müller [46]; Cantor and Teich [47]; Teich, Matin, and Cantor [48]; Teich and Lachs [1])

$$ \bar{n}_c = \frac{\bar{n}_u}{1 + \bar{n}_u(\tau/T)} = \frac{T/\tau}{1 + [\bar{n}_u(\tau/T)]^{-1}} \tag{B.1} $$

and

$$ \sigma_c^2 = \frac{\bar{n}_u}{[1 + \bar{n}_u(\tau/T)]^3} = \frac{(T/\tau)^3 \bar{n}_u^{-2}}{\{1 + [\bar{n}_u(\tau/T)]^{-1}\}^3}, \tag{B.2} $$

respectively. Here $\bar{n}_c$ is the refractoriness-modified mean, σ_c^2 is the refractoriness-modified variance, τ is the dead-time interval, T is the counting-time interval, and $\bar{n}_u$ is the unmodified count mean (which is taken to be directly proportional to the stimulus energy).

For a channel that is sufficiently strongly driven (such that $\bar{n}_u(\tau/T) \gg 1$) we can carry out Taylor series expansions of eqs. (B. 1) and (B. 2) to provide

$$ \bar{n}_c \approx \frac{T}{\tau}\left[1 - \frac{1}{\bar{n}_u(\tau/T)}\right] \tag{B.3} $$

and

$$ \sigma_c^2 \approx \left(\frac{T}{\tau}\right)^3 \frac{1}{\bar{n}_u^2}\left[1 - \frac{3}{\bar{n}_u(\tau/T)}\right] \approx \left(\frac{T}{\tau}\right)^3 \frac{1}{\bar{n}_u^2}. \tag{B.4} $$

The detection law is obtained by considering a fixed detection distance h, such as that represented in eq. (3). The result is in the general form of a ratio of the increment in mean to the standard deviation of the neural count. We therefore form the differential of eq. (B. 3) to obtain

$$ \Delta\bar{n}_c = (T/\tau)^2 \Delta\bar{n}_u/\bar{n}_u^2. \tag{B.5} $$

Then, using eqs. (3), (B.4), (B.5), and the assumption that $\sigma^2(X_s) \approx \sigma^2(X_w)$, we arrive at a single-channel detection distance h_1 given by

$$ h_1 = \Delta\bar{n}_c/\sqrt{2}\,\sigma_c = (1/\sqrt{2})(T/\tau)^{1/2}(\Delta\bar{n}_u/\bar{n}_u). \tag{B.6} $$

The intensity-discrimination law is extracted by forming the logarithm of eq. (B. 6), with the recognition that h_1 is fixed and $\bar{n}_u$ is proportional to the stimulus energy. The treatment is essentially identical to that of van der Velden [4], and the outcome is Weber's Law.

We now strengthen the result by extending it to a collection of k parallel independent neural channels whose outputs (both count means and variances) are summed. Carrying out the summation over the k channels, eq. (B. 5) becomes

$$ \Delta\bar{N}_c = \sum_k \Delta\bar{n}_{ck} = \left(\frac{T}{\tau}\right)^2 \sum_k \frac{\Delta\bar{n}_{uk}}{\bar{n}_{uk}^2}, \tag{B.7} $$

whereas eq. (B.4) becomes

$$ \Sigma_c^2 = \sum_k \sigma_{ck}^2 = \left(\frac{T}{\tau}\right)^3 \sum_k \frac{1}{\bar{n}_{uk}^2}. \tag{B.8} $$

We now let

$$ \bar{n}_{uk} = g(k)\,\bar{n}_u \tag{B.9a} $$

and

$$ \Delta\bar{n}_{uk} = g(k)\Delta\bar{n}_u, \tag{B.9b} $$

where $g(k)$ is the strength of the stimulus as a function of frequency (represented in terms of the channel index k). The detection distance for the overall neural-count random variable is then

$$ h = \frac{\Delta\bar{N}_c}{\sqrt{2}\,\Sigma_c} = \left(\frac{\Delta\bar{n}_u}{\bar{n}_u}\right)\left[\frac{\frac{1}{\sqrt{2}}\left(\frac{T}{\tau}\right)^{1/2}\sum_k \frac{1}{g(k)}}{\left(\sum_k \frac{1}{g^2(k)}\right)^{1/2}}\right]. \tag{B.10} $$

Eq. (B. 10) is similar in form to the single-channel result represented in eq. (B. 6). Both h and the factor in square brackets above are independent of stimulus energy, so that $\Delta\bar{n}_u/\bar{n}_u$ (and therefore $\Delta E/E$) is constant and Weber's Law ensues. We note, however, that the magnitude of the intensity difference limen (DL) will differ in the two cases.

(Received April 15th, 1982.)

References

[1] Teich, M. C. and Lachs, G., A neural-counting model incorporating refractoriness and spread of excitation. I. Application to intensity discrimination. J. Acoust. Soc. Amer. **66** [1979], 1738. This paper is denoted as I in the text.

[2] Lachs, G. and Teich, M. C., A neural-counting model incorporating refractoriness and spread of excitation.

II. Application to loudness estimation. J. Acoust. Soc. Amer. **69** [1981], 774. This paper is denoted as II in the text.

[3] Miller, G. A., Sensitivity to changes in the intensity of white noise and its relation to masking and loudness. J. Acoust. Soc. Amer. **19** [1947], 609.

[4] van der Velden, H. A., Quanteuse verschijnselen bij het zien. Nederlands Tijdschrift voor Natuur Kunde **15** [1949], 147.

[5] Zwicker, E. and Feldtkeller, R., Über die Lautstärke von gleichformigen Geräuschen. Acustica **5** [1955], 303.

[6] Feldtkeller, R. and Zwicker, E., Das Ohr als Nachrichtenempfänger (S. Hirzel-Verlag, Stuttgart 1956) p. 82.

[7] Zwicker, E., Flottorp, G., and Stevens, S. S., Critical bandwidth in loudness summation. J. Acoust. Soc. Amer. **29** [1957], 548.

[8] Fletcher, H., Auditory patterns. Revs. Mod. Phys. **12** [1940], 47.

[9] Scharf, B., Loudness of complex sounds as a function of the number of components. J. Acoust. Soc. Amer. **31** [1959], 783.

[10] Scharf, B., "Loudness", in Handbook of Perception, Vol. IV, Hearing, E. C. Carterette and M. P. Friedman, Eds., Academic, New York 1978, pp. 187–242.

[11] Zwislocki, J., "Masking: Experimental and theoretical aspects of simultaneous, forward, backward, and central masking", in Handbook of Perception, Vol. IV, Hearing, E. C. Carterette and M. P. Friedman, Eds., Academic, New York 1978, pp. 283–336.

[12] Brittain, F. H., The loudness of continuous spectrum noise and its application to loudness measurements. J. Acoust. Soc. Amer. **11** [1939], 113.

[13] Stevens, S. S., The measurement of loudness. J. Acoust. Soc. Amer. **27** [1955], 815.

[14] Zwicker, E., Über psychologische und methodische Grundlagen der Lautheit. Akust. Beih. Acustica **1** [1958], 237.

[15] Zwicker, E., "Scaling", in Handbook of Sensory Physiology, Auditory System, edited by W. D. Keidel and W. D. Neff, Springer-Verlag, Berlin 1975, Vol. V/2, pp. 401–448.

[16] Hawkins, J. E., Jr. and Stevens, S. S., The masking of pure tones and of speech by white noise. J. Acoust. Soc. Amer. **22** [1950], 6.

[17] Zwicker, E., Die elementaren Grundlagen zur Bestimmung der Informationskapazität des Gehörs. Acustica **6** [1956], 365.

[18] Bos, C. E. and de Boer, E., Masking and discrimination. J. Acoust. Soc. Amer. **39** [1966], 708.

[19] Raab, D. H. and Goldberg, I. A., Auditory intensity discrimination with bursts of reproducible noise. J. Acoust. Soc. Amer. **57** [1975], 437.

[20] Rabinowitz, W. M., Lim, J. S., Braida, L. D., and Durlach, N. I., Intensity perception. VI. Summary of recent data on deviations from Weber's law for 1000-Hz tone pulses. J. Acoust. Soc. Amer. **59** [1976], 1506.

[21] Jesteadt, W., Wier, C. C., and Green, D. M., Intensity discrimination as a function of frequency and sensation level. J. Acoust. Soc. Amer. **61** [1977], 169.

[22] Green, D. M., Auditory detection of a noise signal. J. Acoust. Soc. Amer. **32** [1960], 121.

[23] Jeffress, L. A., Stimulus-oriented approach to detection. J. Acoust. Soc. Amer. **36** [1964], 766.

[24] Pfafflin, S. M. and Mathews, M. V., Detection of auditory signals in reproducible noise. J. Acoust. Soc. Amer. **39** [1966], 340.

[25] de Boer, E., Intensity discrimination of fluctuating signals. J. Acoust. Soc. Amer. **40** [1966], 552.

[26] McGill, W. J., Neural counting mechanisms and energy detection in audition. J. Math. Psychol. **4** [1967], 351.

[27] Ronken, D. A., Intensity discrimination of Rayleigh noise. J. Acoust. Soc. Amer. **45** [1969], 54.

[28] Teich, M. C. and McGill, W. J., Neural counting and photon counting in the presence of dead time. Phys. Rev. Lett. **36** [1976], 754, 1473.

[29] Green, D. M. and Swets, J. A., Signal Detection Theory and Psychophysics. Wiley, New York 1966. [Reprinted 1974. (Robert E. Krieger Publishing Co., Huntington, New York)].

[30] Bouman, M. A., Vos, J., and Walraven, P., Fluctuation theory of luminance and chromaticity discrimination. J. Opt. Soc. Amer. **53** [1963], 121.

[31] Penner, M. J. and Viemeister, N. F., Intensity discrimination of clicks: The effects of click bandwidth and background noise. J. Acoust. Soc. Amer. **54** [1973], 1184.

[32] Viemeister, N. F., Intensity discrimination of noise in the presence of band-reject noise. J. Acoust. Soc. Amer. **56** [1974], 1594.

[33] Moore, B. C. J. and Raab, D. H., Intensity discrimination for noise bursts in the presence of a continuous, bandstop background: Effect of level, width of the bandstop, and duration. J. Acoust. Soc. Amer. **57** [1975], 400.

[34] Viemeister, N. F., Intensity discrimination of pulsed sinusoids: The effects of filtered noise. J. Acoust. Soc. Amer. **51** [1972], 1265.

[35] Moore, B. C. J. and Raab. D. H., Pure-tone intensity discrimination: Some experiments relating to the "near-miss" to Weber's Law. J. Acoust. Soc. Amer. **55** [1974], 1049.

[36] Spiegel, M. F. and Green, D. M., Two procedures for estimating internal noise. J. Acoust. Soc. Amer. **70** [1981], 69.

[37] Prucnal, P. R. and Teich, M. C., An increment threshold law for stimuli of arbitrary statistics. J. Math. Psychol. **21** [1980], 168.

[38] Sorkin, R. D., Woods, D. D., and Boggs, G. J., Signal detection in computer-synthesized noise. J. Acoust. Soc. Amer. **66** [1979], 1351.

[39] Papoulis, A., Probability, Random Variables, and Stochastic Processes. McGraw-Hill, New York 1965.

[40] Siebert, W. M., "Stimulus transformations in the peripheral auditory system", in Recognizing Patterns, P. A. Kolers and M. Eden, Eds. MIT Press, Cambridge, MA 1968, pp. 104–133.

[41] Vannucci, G. and Teich, M. C., Dead-time-modified photocount mean and variance for chaotic radiation. J. Opt. Soc. Amer. **71** [1981], 164.

[42] Zwicker, E. and Scharf, B., A model of loudness summation. Psychol. Rev. **72** [1965], 3.

[43] Teich, M. C. and Diament, P., Relative refractoriness in visual information processing. Biol. Cybern. **38** [1980], 187.

[44] Teich, M. C. and Lachs, G., A neural-counting model incorporating refractoriness and spread of excitation: Application to intensity discrimination and loudness estimation for variable-bandwidth noise stimuli, (Abstract). J. Acoust. Soc. Amer. **69** [1981], S104.

[45] Gradshteyn, I. S. and Ryzhik, I. M., Tables of Integrals, Series, and Products; translation edited by A. Jeffrey, Academic, New York 1965.
[46] Müller, J. W., Some formulae for a dead-time-distorted Poisson process. Nucl. Instrum. Methods **117** [1974], 401.
[47] Cantor, B. I. and Teich, M. C., Dead-time-corrected photocounting distributions for laser radiation. J. Opt. Soc. Amer. **65** [1975], 786.
[48] Teich, M. C., Matin, L., and Cantor, B. I., Refractoriness in the maintained discharge of the cat's retinal ganglion cell. J. Opt. Soc. Amer. **68** [1978], 386.